Received: 12 June 2019 | Revised: 29 August 2019 | Accepted: 12 September 2019

DOI: 10.1002/apj.2374

RESEARCH ARTICLE

WILEY Asia-Pacific Journal of Chemical Engineering | Curtin University

Newly designed bioanode for glucose/O_2 biofuel cells to generate renewable energy

Seyda Korkut[1] | Muhammet Samet Kiliç[2] | Baki Hazer[3,4]

[1]Department of Environmental Engineering, Zonguldak Bulent Ecevit University, Zonguldak, Turkey

[2]Department of Biomedical Engineering, Zonguldak Bulent Ecevit University, Zonguldak, Turkey

[3]Department of Chemistry; Department of Aircraft Airframe Engine Maintenance, Kapadokya University, 50420 Ürgüp, Nevşehir, Turkey

[4]Department of Nanotechnology Engineering, Zonguldak Bulent Ecevit University, 67100 Zonguldak, Turkey

Correspondence
Seyda Korkut, Department of Environmental Engineering, Zonguldak Bulent Ecevit University, 67100, Zonguldak, Turkey.
Email: s.korkut@beun.edu.tr

Funding information
Zonguldak Bulent Ecevit University, Grant/Award Number: BEU-2013-77047330-01; Bulent Ecevit University Research Fund, Grant/Award Number: BEU-2013-77047330-01; Scientific & Technological Research Council of Turkey (TUBITAK), Grant/Award Number: 112Y100

Abstract

A copolymer poly(methyl methacrylate-*co*-vinylferrocene) was synthesized and used for the first time in a biofuel cell design. Bioanaode enzyme glucose oxidase and biocathode enzyme bilirubin oxidase were physically immobilized onto the copolymer-modified electrodes. Characterization studies were conducted by scanning electron microscopy, carbon-13, fourier transform infrared and hydrogen-1 nuclear magnetic resonance, and cyclic voltammograms. The designed biofuel cell was operated with linear sweep voltammetry. The maximum current was at 45°C with 120 μg of polymer amount. An improved power density of 323 μW cm^{-2} that is higher than other ferrocene-based fuel cells was obtained with 10-mM glucose at 0.4 V with the designed bioanode.

KEYWORDS

biofuels, electrochemistry, fuel cell, renewable energy

1 | INTRODUCTION

Biofuel cells are commonly based on microbial and enzymatic working electrodes. Microbial cells have the superiority of being able to catalyze the complete oxidation of biofuels and have long lifetimes (up to 3–5 years) but are plagued by low power density (1–90 μW cm^{-2}).[1] Enzyme-based fuel cell (EFC) is an eco-friendly and compact power supply that generates electrical energy from the natural fuels by utilizing the enzymes as electrocatalysts.[2] However, it suffers from inefficient electron transport between the biomolecule and electrode because the active center of the biomolecule is deeply buried in the protein shell.[3] To overcome this drawback, it should be especially focused on designing of bioanode that is responsible for the fuel oxidation for construction of the EFC to improve generated power with a high catalytic current density. Enzyme glucose oxidase (GOx) is commonly used for bioanode because it offers relatively low cofactor redox potential.[4] But a proper redox mediator is needed due to its nonconductive protein shell that covers the active site as well as the redox center for shuttling the electrons between electrode and enzyme. Researchers have been working to accelerate the electron transfer rate on the electrode surfaces in recent years. For this purpose, conductive nanoparticles[5-7] and mediator-

modified working electrodes such as carbon nanotubes,[8,9] osmium complexes,[10] *p*-benzoquinone,[11] and 2,2′-azino-bis(3-ethyl benothiazoline-6-sulfonate)[12] have been developed and used. Among the numerous mediators, ferrocene plays an important role. Ferrocene containing two cyclopentadienyl ligands that were bound on the opposite sides of a central Fe(II) atom [$Fe(C_5H_5)_2$] is an organometallic substance. It presents excellent electrochemical characteristics, a one electron transfer to/from ferrocene/ferrocenium that is typically rapid, because of the low reorganization energy of the Fe(II) and Fe(III) redox states.[13]

Up to now, poly(vinylferrocene) (PVFc) containing polymers have gained attention due to redox activity, and chemically stable materials are attained by placing the ferrocenyl groups in other chains.[14] In the study of synthesizing these kinds of polymers, Nunns et al.[15] achieved to synthesize a large number of those with unprecedented characteristics. Tonhauser et al.[16] reported the synthesis of the first amphiphilic PVFc containing copolymers. Conducting polymer composites of PVFc and polypyrrole were synthesized in another report,[17] and the results showed that PVFc containing composites were more stable than the homopolymer of PVFc. The copolymers of vinylferrocene such as poly (vinylferrocene-*co*-hydroxyethyl methacrylate),[18] poly (glycidyl methacrylate-*co*-vinylferrocene),[19] acrylamide copolymers,[20] and poly(N-acryloylpyrrolidine-*co*-vinylferrocene)[21] were used in sensor studies and resulted in successful signals. Although such good results were achieved by using these polymers, as far as we know, PVFc and its copolymers have not been used for an EFC design yet. In this report, poly(methyl methacrylate-*co*-vinylferrocene) was synthesized by free radical polymerization and used for the first time in design of the EFC system to acquire a biocompatible polymer and accelerated electron transfer on the gold surface. The bioelectrode performance was tested with different temperature and various polymer amounts. The power generation efficiency of the designed EFC used glucose as fuel was investigated.

2 | MATERIALS AND METHODS

2.1 | Reagents

Methyl methacrylate (99%), vinylferrocene (97%), azobisisobutyronitrile, chloroform (≥99% GC grade), tetrahydrofurane (99.9% GC grade), diethyl ether (99.7%), acetonitrile (99.9% GC grade), GOx from Aspergillus niger (10 kU), bilirubin oxidase from Myrothecium verrucaria (25 U; BOD), and glucose monohydrate were bought from Sigma-Aldrich. Potassium dihydrogen phosphate and dipotassium hydrogen phosphate were obtained from Merck. Enzyme and glucose stock solutions were freshly prepared in 100 mM, pH 7.4 phosphate buffer for EFC experiments.

2.2 | Chemical synthesis of poly(methyl methacrylate-co-vinylferrocene)

Poly(methyl methacrylate-*co*-vinylferrocene) [poly(MMA-*co*-VFc)] was synthesized by free radical polymerization technique.[22] The synthesis reaction was initiated by dissolving 1.2 g of methyl methacrylate, 1 g of vinylferrocene (VFc), and 0.04 g of azobisisobutyronitrile (initiator) in 10 ml of freshly distilled chloroform by mixing the reaction medium at room temperature under argon medium. The polymerization reaction was carried out in oil bath at 70°C for 2 hr afterwards. Synthesized polymer was precipitated in diethyl ether. The polymer was filtered and then washed with ultrapure water, dried in vacuum oven at 50°C for 1 day. It was redissolved and reprecipitated in tetrahydrofuran and in 100 ml of diethyl ether, respectively for the purification. Finally, it was again dried under vacuum overnight at 50°C. A 10 mg ml^{-1} of the resulting poly(MMA-*co*-VFc) solution was prepared in tetrahydrofuran to use for electrode coating. Hydrogen-1 (^{1}H-NMR) and carbon-13 nuclear magnetic resonance spectroscopy (^{13}C-NMR) spectra of the samples were charted using a Bruker Minispec Pulsed Spectrometer in cadmium chloride solvent and tetramethylsilane internal standard. Fourier transform infrared spectroscopy (FT-IR) spectrums were recorded with the Perkin Elmer Spectrum 100 spectrometer.

2.3 | Electrochemical apparatus and biofuel cell operation

CH Instruments 1040B electrochemical analyzer was used for enzymatic fuel cell experiments. Gold (diameter = 2 mm) working electrodes, wire platinium that was used as the counter electrode, reference electrode (Ag/AgCl), and the electrochemical cell were supplied from CH Instruments. To design a glucose/O_2 biofuel cell, poly (MMA-*co*-VFc)/GOx and poly(MMA-*co*-VFc)/BOD biofilm modified gold electrode was used as the bioanode and the biocathode, respectively. The biofuel cell compartment was filled with the aerated 100 mM, pH 7.4 phosphate buffer. The four-electrode system was immersed into the compartment, and the biofuel cell was operated by using linear sweep voltammetry technique (LSV) at a potential scan between −1 and +1 V. The power density was measured as explained previously.[23]

The schematic setup and electrochemical reactions of the biofuel cell were presented in Scheme 1. In this setup, enzyme GOx responsible for the oxidation of glucose is immobilized onto the poly(MMA-*co*-VFc)-coated anode side, whereas BOD is immobilized onto the cathode prepared with the same polymer. When glucose is added into the solution, it is oxidized by the bioanode, then released electrons are moved to the biocathode side under a suitable potential. Molecular oxygen is reduced by BOD on the cathode surface with this electron flow. As long as the enzyme reactions continue on the anode and cathode surfaces, this continuous electron flow generates an electric current in the circuit.

2.4 | Fabrication of the biofuel cell electrodes

The gold electrodes were polished with slurries of fine containing alumina powders of 0.05, 0.3, and 1 micron on a polishing microcloth pad. Then, the electrodes were flushed with ultrapure water. At the final cleaning step, cyclic voltammograms of the gold electrodes at a potential scan ranging between −1 and +1 V with a scan rate of 50 mV s^{-1} in phosphate buffer solution were conducted. A 12 μL of the 10-mg ml^{-1} poly (MMA-*co*-VFc) solution was spread directly onto the pretreated surface of the gold anode and cathode, then waited at room temperature to evaporate solvent. The working electrodes were immersed in ultrapure water prior to the enzyme immobilization. A 10 μL of GOx (10 mg ml^{-1}) and 10 μL of BOD was dropped onto the poly(MMA-*co*-VFc) thin film-coated anode and cathode, respectively. The working electrodes were waited for physical immobilization of the enzymes at room temperature for 2 hr and rinsed with phosphate buffer to remove free enzyme on the electrode surfaces.

3 | RESULTS AND DISCUSSION

3.1 | Material characterization and surface morphology

Poly(MMA-*co*-VFc) was characterized by using ^{1}H-NMR and ^{13}C-NMR, scanning electron microscope (SEM), and FT-IR. The methoxy group of the poly(methyl methacrylate) at 3.5 ppm and aromatic pentadienyl cycle of ferrocene at 4.1 ppm were observed in ^{1}H-NMR spectrum (Figure S1a). Aromatic pentadienyl cycle of ferrocene was also determined at 69 ppm and carbonyl group (−C═O) of poly(methyl methacrylate) was observed at 178 ppm in the 13C-NMR spectrum (Figure S1b). The FT-IR spectrum was presented in Figure S2. The characteristic signals of carbonyl group of poly(methyl methacrylate) were observed at 1724.96 cm^{-1}. The strong signals of ferrocene rings and −C—H stretching of aromatic pentadienyl cycle of PVFc were observed at 1036.30 and 3332.67 cm^{-1}, respectively. It was understood from the spectrums that the desired copolymer was successfully synthesized.

SEM images of poly(MMA-*co*-VFc) in Figure 1a, GOx immobilized poly(MMA-*co*-VFc) in Figure 1b, and BOD immobilized poly(MMA-*co*-VFc) in Figure 1c coated electrode surfaces were taken with Quanta FEG 450 SEM device. The poly(MMA-*co*-VFc) film-coated electrode was compact and uniform, which was beneficial for the adequate adsorption of enzyme molecules. It was

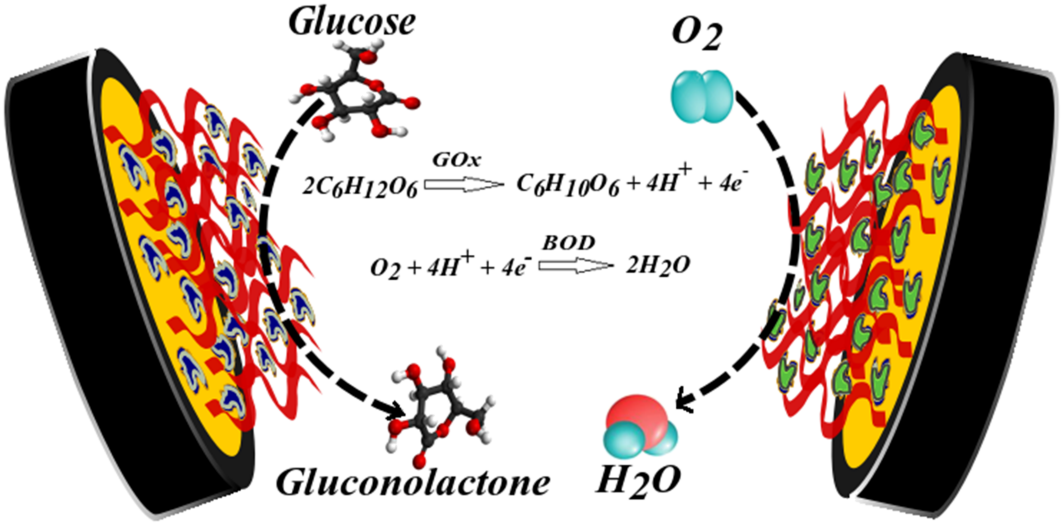

SCHEME 1 The schematic diagram of the EFC with the surface reactions

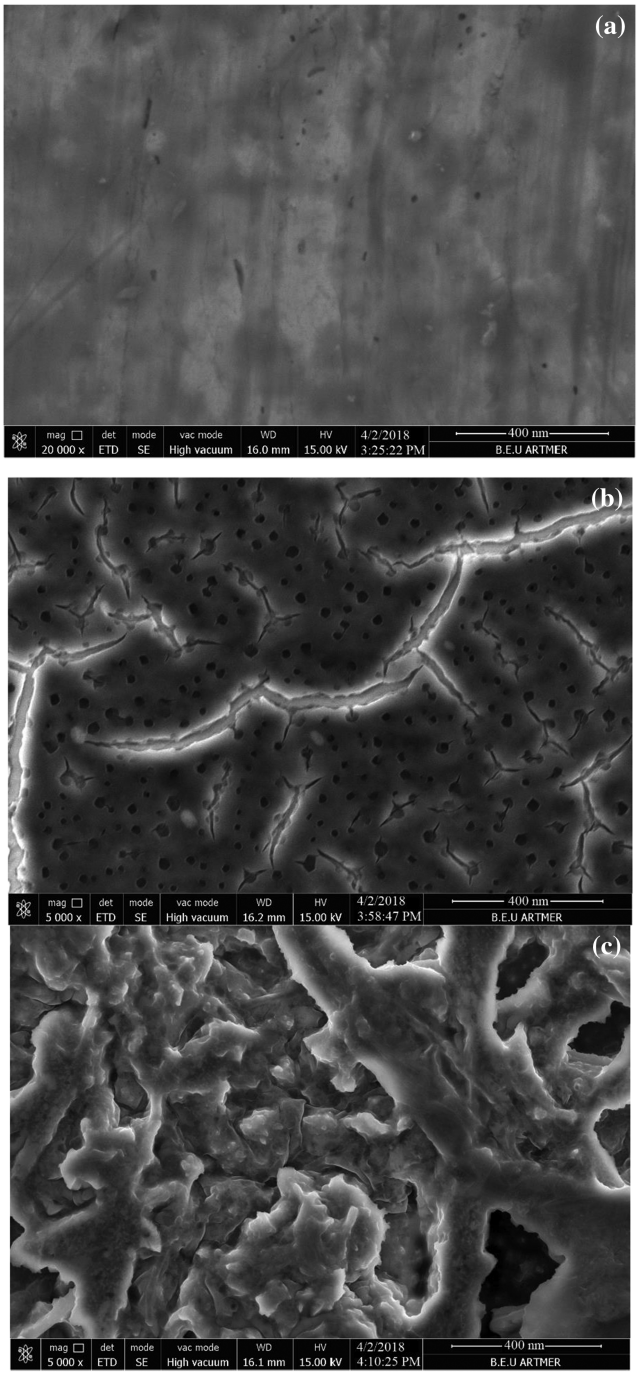

FIGURE 1 (a) Scanning electron microscope of the poly(MMA-*co*-VFc), (b) poly(MMA-*co*-VFc)/glucose oxidase, and (c) poly (MMA-*co*-VFc)/bilirubin oxidase film-coated electrode surface at a magnification of the 400 nm

observed that surface morphology was altered due to adsorption and coverage of enzyme molecules over the poly(MMA-*co*-VFc) film. Grain and circular enzyme clusters were observed from the SEM image of the poly (MMA-*co*-VFc)/GOx electrode as a result of GOx adsorption. The previously published SEM images of GOx were similar in appearance.[24,25]

3.2 | Electrochemical characterization

Poly(MMA-*co*-VFc)/GOx bioanode was characterized using the cyclic voltammetry (CV) technique by operating three-electrode system in 100 mM, pH 7.4 phosphate buffer containing 10 mM of $K_3Fe(CN)_6$. The scan rate dependence cyclic voltammetric response of the bioanode in the potential range of 80 to 500 mV s^{-1} for the redox reactions of $Fe(CN)_6^{-3}/Fe(CN)_6^{-4}$ on the bioelectrode was shown in Figure S3a (The inner CVs represented the slowest scan rate). The peak currents changed linearly by the square root of the scan rate over the range of 80 to 500 mV s^{-1} (Figure S3b), suggesting diffusion controlled mass transfer reactions and reversible system. In reversible systems, the current of the peak is given by Randles–Sevcik equation that is used to determine the electron diffusion coefficient in the polymeric film layer:

$$I_p = \left(2.69 \times 10^5\right) \times n^{3/2} \times A \times D_e^{1/2} \times C \times v^{1/2} \quad (1)$$

where I_p is the peak current, A; n is the electrons involved; A is the electrode area, cm^2; D is the diffusion coefficient, $cm^2\ s^{-1}$; C is the concentration, mol cm^{-3}; and v is the scan rate, V s^{-1}. Thus I_p rises with square root of *v* and is directly proportional to substances concentrations. The electron diffusion coefficient (D_e) in the polymeric layer was calculated from the slope of the linear curve. The regression equation was $y = 0.0002x - 9.10^{-7}$ ($r^2 = .999$) for the oxidation currents and $y = -0.0002x - 9.10^{-6}$ ($r^2 = .997$) for the reduction currents. D_e was found to be 5.62×10^{-6} $cm^2\ s^{-1}$.

To investigate the electrochemical characterization of VFc unit, a CV experiment was conducted by using a bare gold electrode in VFc solution. Figure S4 shows the CVs of the bare gold electrodes in acetonitrile (A), in 2-μM VFc solution prepared with acetonitrile (B) at 100 mV s^{-1} scan rate (vs. Ag^0/Ag^+). As expected, no redox peaks were observed on the curve (A), whereas the cathodic peak displaying on the curve (B) between −0.2 and −0.4 V was directly related to VFc unit in the solution. Initially, the ferric ion exists in both the oxidized form Fe(III) and the reduced form Fe(II) in VFc.[26] The electrochemical behavior of the bare gold and poly(MMA-*co*-VFc)/GOx biofilm-coated gold surface was investigated in phosphate buffer by CV at 100 mV s^{-1} scan rate (vs. Ag/AgCl). In Figure 2, the typical CV of VFc unit at negative potentials was observed for Au/poly(MMA-*co*-VFc)/GOx electrode. The voltammetric behavior indicated that the gold electrode surface was successfully covered by copolymer with VFc unit. In addition, the copolymer coated surface caused an increase in current density compared with the bare gold surface. The reduction peak observed for the copolymer coated surface at +0.4 V was

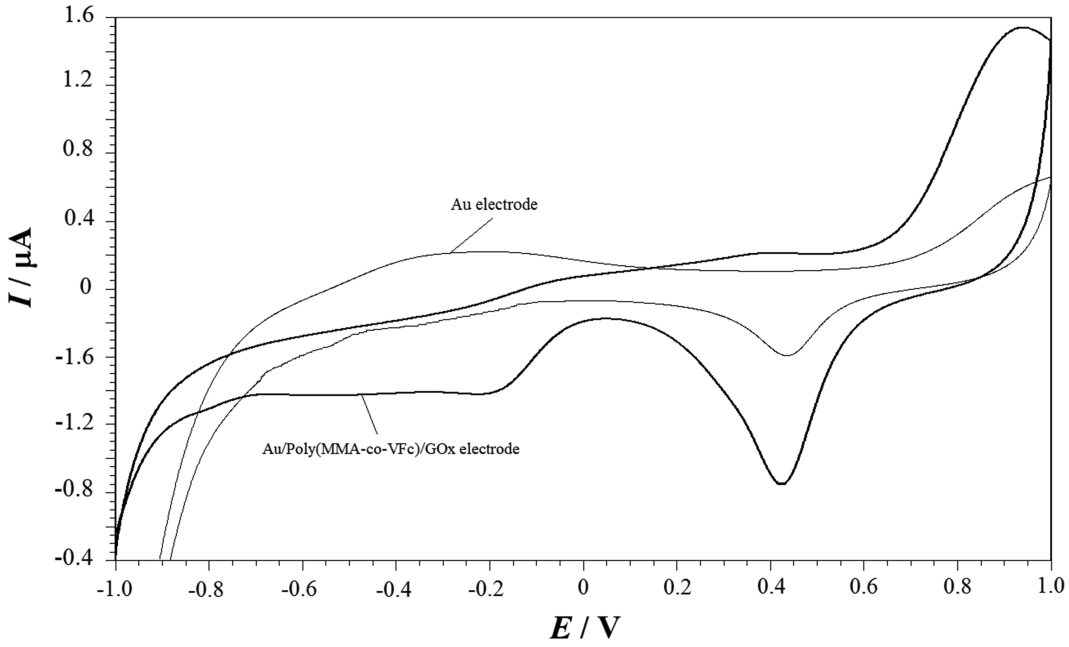

FIGURE 2 CV of the bare gold and poly(MMA-*co*-VFc)/GOx film-coated gold electrode in 10 ml of phosphate buffer at a potential scan ranging between −1 V and +1 V (vs. Ag/AgCl) with a scan rate of 100 mV s^{-1}

due to the bare gold electrode, not the polymer, because it was observed in the CV of the bare gold electrode.

3.3 | Effective polymer mass for enhanced fuel oxidation

An important role of the polymeric layer used as support material is to protect the active sites of the enzyme from the adverse effects of the components of the reaction mixture and the processing conditions. The greatest advantage of polymeric film is that it can be synthesized freely and modified according to the enzyme requirements and the process used in biological fuel cells and biosensors.[27] However, even if the desired polymer is synthesized, the increasing density of polymer on electrode surface may slow/hinder electron flow because it is an obstacle to mass transfer. Therefore, the polymer density on the electrode surface should be optimized to obtain an effective power generation from the EFC. Poly(MMA-*co*-VFc)/GOx bioanode surfaces were prepared at various amounts of polymer ranging between 20, 40, 50, 120, and 180 μg [2, 4, 5, 12, and 18 μL of poly (MMA-*co*-VFc)]. A 10 μL of GOx (10 mg ml^{-1}) was dropped onto the each bioanode. The prepared bioanodes were tested in 10 ml of aerated phosphate buffer containing 3-mM glucose with using LSV technique at a potential scan between −1 and +1 V with a scan rate of 100 mV s^{-1}. The anodic currents obtained from LSV technique were presented in Figure 3. The current increased with the increasing amount of polymer reached to the highest value at 120 μg of polymer amount and then decreased after exceeding this quantity. It was understood from Figure 3 that an internal diffusion barrier originating from the polymer density limited the electron transfer realized on the electrode surface through the electrochemical process beyond 120 μg of poly(MMA-*co*-VFc) quantity. In another perspective, an internal diffusion barrier in which the enzyme is present inside the polymeric film, it can limit diffusion of substrate molecules into the polymer.[28]

3.4 | Temperature test

The temperature effect can be particularly important for enzymatic systems in which the activity and durability of biocatalysts are generally maximized in a very strict temperature range.[29] Enzymes are denatured at very high temperatures, the enzyme and substrate can not complement each other, resulting in a lower reaction rate. To investigate the effect of temperature on the biofuel cell electrodes, four series of biofuel cell comprised 120 μg of poly(MMA-*co*-VFc)-coated anodes and cathodes were prepared. A 10 μL of GOx (10 mg ml^{-1}) was dropped onto the surface of the polymeric film modified anode, and 10 μL of BOD (10 mg ml^{-1}) was dropped onto the modified cathode. The prepared biofuel cells were operated at 0.4 V in a 500-μM glucose solution prepared with aerated phosphate buffer at 25, 35, 45, and 55°C. Corresponding current-temperature graph of the bioanode and the

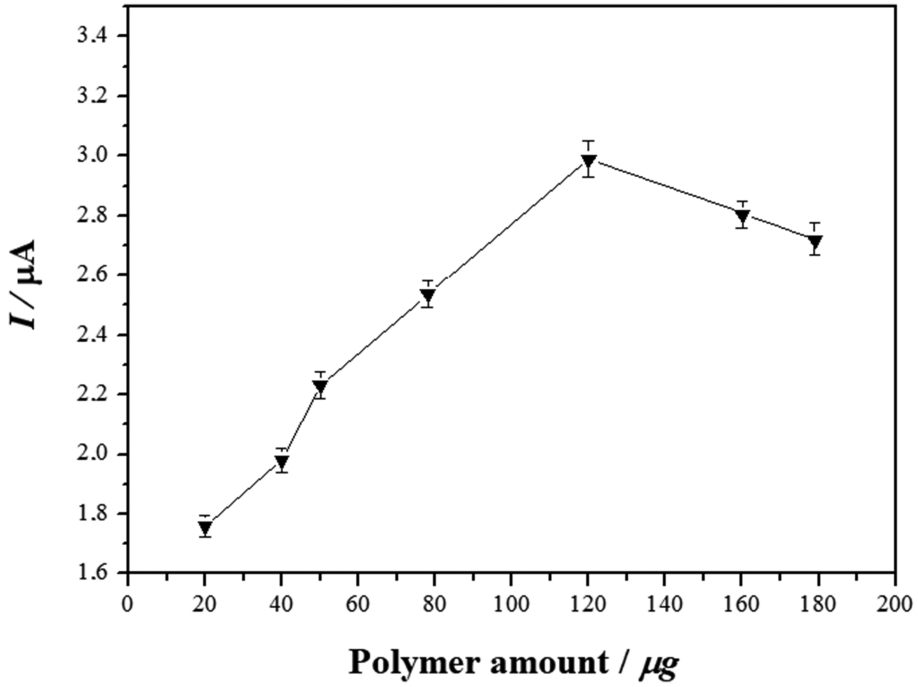

FIGURE 3 The current performances obtained from the bioanodes fabricated with various polymer amounts with 10-mM glucose

biocathode was presented in Figure 4. It was observed that the maximum current value was reached at 45°C for each two electrodes. Excessive increase in temperature leaded to a reduction in the signal of the electrodes, which was because the thermal degradation of the enzyme. The designed biofuel cell was operated at room temperature because the long-term operation of the biofuel cell at such a high temperature can damage the enzymes. In addition, in vivo applications are based on the fact that enzymatic fuel cells have the ability to operate optimally at temperatures between room temperature and body temperature.

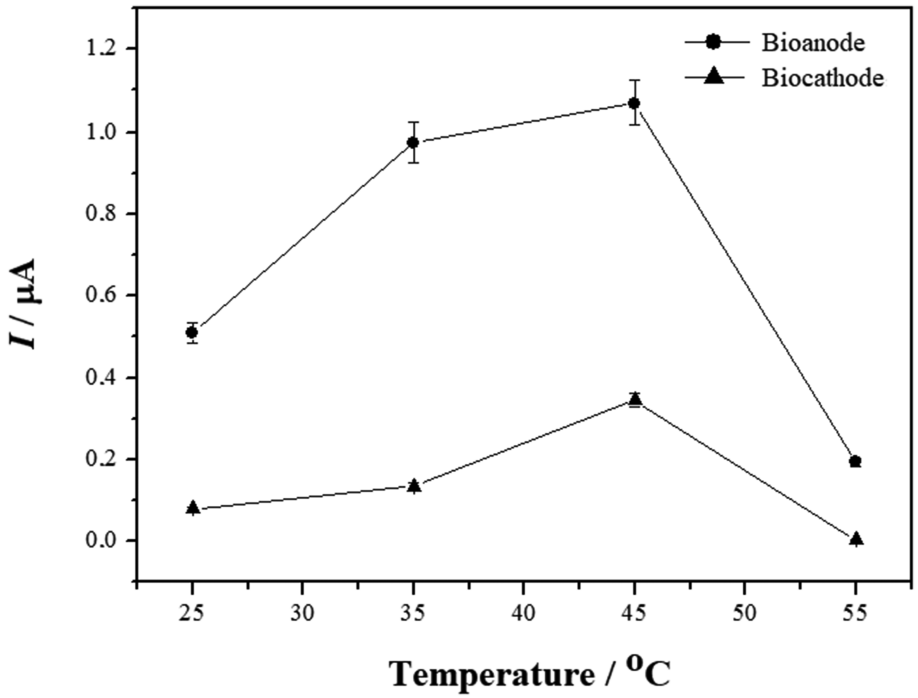

FIGURE 4 Effect of temperature on the efficiency of bioanode and biocathode in enzyme-based fuel cell

3.5 | Performance of the bioanode and the biofuel cell

To investigate the fuel oxidation performance of the bioanode, LSVs of poly(MMA-*co*-VFc)/GOx electrode were recorded in air-saturated buffer solution containing glucose at varied concentrations ranging between 1 and 40 mM at 100 mV s^{-1} scan rate. The obtained anodic peak currents were presented in Figure 5a. The electron transfer process of GOx is a two electron and two proton-dependent reactions, and the peak current of the anode is attributed to oxidation of $FADH_2$ placed in the redox active center of GOx.[30] In the system, as the oxidation of glucose increases, more reduced $FADH_2$ are formed, resulting in more $FADH_2$ being oxidized on the anode surface with the increasing glucose. As seen in Figure 5a, the oxidation current increased gradually and linearly ($y = 0.4562x + 1.9023$, $r^2 = .991$; Figure 5b), which could be attributed to the GOx-catalyzed glucose oxidation (Scheme 1), with the increasing glucose concentration. This current increase tendency in a large fuel range probably will lead to result in higher power output for the designed EFC. The performance of the EFC comprised the poly(MMA-*co*-VFc)/GOx bioanode and poly(MMA-*co*-VFc)/BOD biocathode was further investigated with LSV under the optimum conditions to characterize power output of the system[31] in presence of 10-mM glucose. First, the current density (I, μA cm^{-2}) − voltage (V, Volt) curves were obtained, then they were converted to the power density (P, μW cm^{-2}) − voltage curves in accordance with $P = I \times V$ equation.[32] The generated power (P, μW) was divided over the active surface area for calculation of the power density. The power density as a function of the cell voltage for the EFC operated at room temperature was presented in Figure 6. The ultimate power density was found to be 323 μW cm^{-2} at 0.4 V, which was superior to those previously reported ferrocene-containing redox polymer-based fuel cell electrodes using poly(N-(3-dimethyl (ferrocenyl) methylammoniumbromide) propylacrylamide) that was used to improve the efficiency of current generation in a GOx modified anode (1.7 μW cm^{-2} at 0.27 V),[33] ferrocene-modified linear poly(ethyleneimine) utilized as fructose dehydrogenase

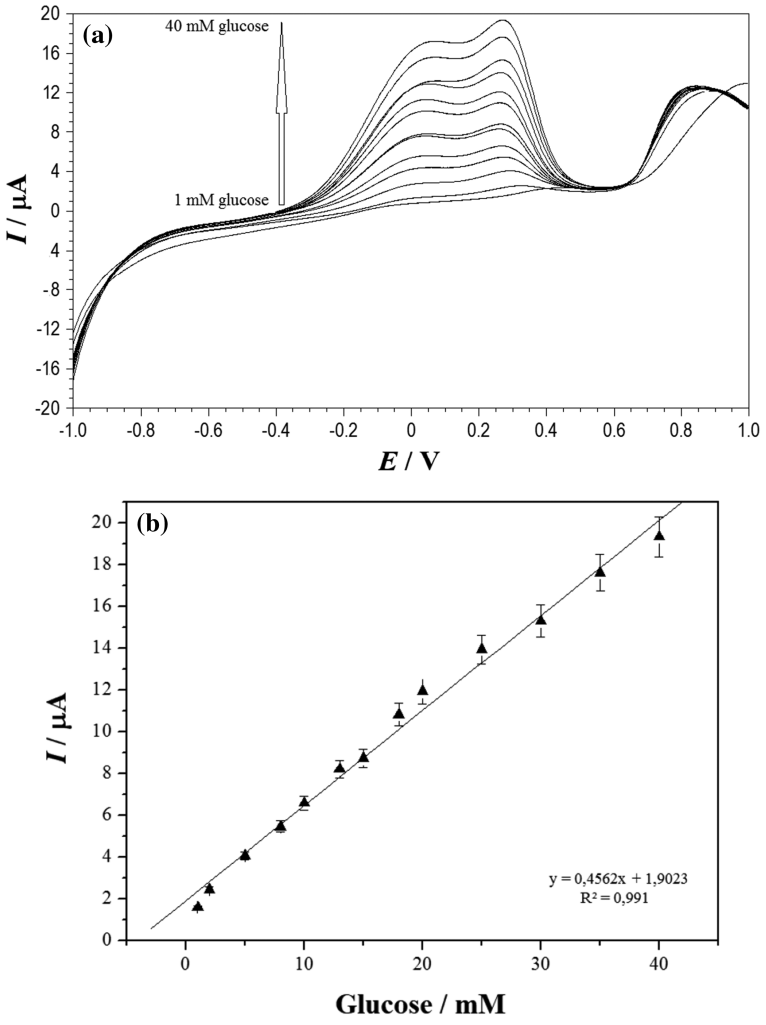

FIGURE 5 (a) Linear sweep voltammogram of the bioanode calibration to increasing glucose concentrations ranging between 1 and 40 mM in phosphate buffer at a potential scan ranging between −1 and +1 V (vs. Ag/AgCl) with a scan rate of 100 mV s^{-1} and (b) calibration curve obtained from linear sweep voltammogram in linear range from 1 to 40 mM.

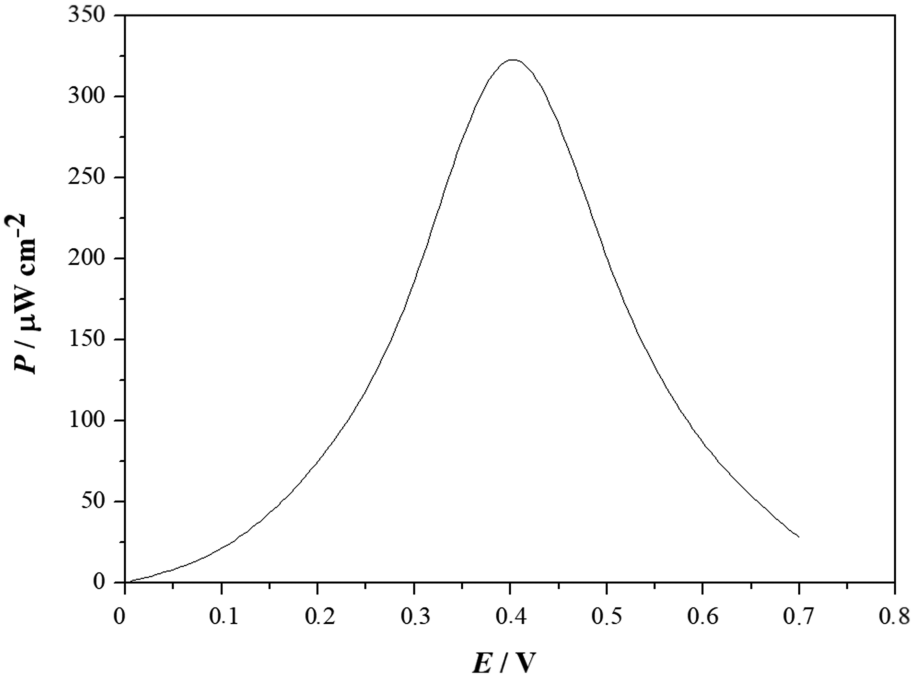

FIGURE 6 Effect of cell voltage on power density (obtained from biocathode) of the enzyme-based fuel cell

immobilized bioanode in an enzymatic fuel cell (29 μW cm^{-2}).[34] In another study, ferrocene-modified solid binding matrix/graphite composite film was used as GOx-based anode and horseradish peroxidase-based cathode. The composite material was placed layer-by-layer on a large polymeric surface. The electrodes were assembled into a biofuel cell, which utilized glucose as fuel and hydrogen peroxide as oxidizer. The power output of the cell was 0.15 μW cm^{-2} at 0.021 V.[35] A membraneless biofuel cell was prepared based on GOx anode and laccase cathode by using 1,1′-dicarboxyferrocene as the mediator. Grape, banana, and orange juice containing glucose were used as the fuel. The system generated the highest power density of 28.4 μW cm^{-2}.[36] The power densities obtained from the previous paper were presented in Table 1.

3.6 | Operational stability, reproducibility, and wastewater test of the bioanode

The operational stability of a new freshly prepared poly (MMA-*co*-VFc)/GOx bioanode was investigated. Figure S5 shows the 50 cycles CVs of the bioanode in the air-saturated phosphate buffer at 100 mV s^{-1} scan rate. After 50 cycles, the redox peaks directly related to VFc unit were still obvious. The peak currents were the same up to 38 cycles, declined only about 7 μA at the last 12 cycles, indicating that the fabricated electrode was highly stable. Five different poly(MMA-*co*-VFc)/GOx bioanode were prepared to determine if the prepared electrode was reproducible and each of these electrodes was tested on Days 1, 2, 3, 4, and 7 (5 days). CVs of each prepared bioanode in the air-saturated phosphate buffer at a scan rate of 100 mV s^{-1} were shown in Figure S6a–e. Figure S6 showed that the current values obtained from different electrodes were the same. The relative standard deviation (RSD %) of the current values obtained from 5 days usage of each electrode varied between 0.7% and 1.35% (Figure S6f). The low standard deviation of the current values obtained from interday usage of five different electrodes prepared under the same conditions indicated that the storage time period of the bioanode might be longer than 5 days, and the proposed electrode is highly reliable and reproducible.

The bioanode performance of the designed EFC was tested with a municipal wastewater sample collected from the aeration reactor of the Biological Treatment Plant in Zonguldak City. The sample was filtered with a Whatman membrane filter (0.2 μm) to eliminate microorganisms and other particules and then 200 μL of the filtered sample was added into the 10 ml of air-saturated buffer. EFC was operated in this solution at a fixed potential of 0.25 where glucose oxidation was observed (as seen in Figure 5a). The amperometric current-time graph was presented in Figure S7. An oxidation current of 0.6 μA was observed on the bioanode by the addition of the 50-fold diluted wastewater sample. The bioanode presented a reasonable and high current density of 955 μA cm^{-2} for the real municipal wastewater, this result showed that

TABLE 1 Power densities of the previously published enzyme-based fuel cells

Electrode	Fuel (glucose; mM)	Power density ($\mu W/cm^2$)	Reference
3-(dimethylferrocenyl)propyl-linear poly (ethylenimine)	60	146	37
*[poly(3-aminobenzoicacid-co-2-methoxyaniline-5-sulfonicacid) based buckypaper electrode *[poly(3-aminobenzoicacid-co-2-methoxyaniline-5-sulfonicacid) based vertically aligned carbon nanotubes electrode	10	107 122	9
Carbon nanotubes-hydroxyapatite nanocomposite	10	15.8	38
ZnO-ferrocene/multiwalled carbon nanotubes/nafion Ferrocene/carbon nanotubes	50	53 13	39
Poly(4-vinylpyridine)[Os(N,N′-dimethyl-2,2′-biimidazole)3]$^{2+/3+}$)	15	350	40
Multiwalled carbon nanotube buckypaper	Human serum + 20-mM glucose	49.16	41

the system utilized glucose content of the wastewater effectively to generate power.

4 | CONCLUSION

Poly(MMA-*co*-VFc) copolymer was chemically synthesized and first time used as electrode surface material for a biofuel cell development. Based on the poly (MMA-*co*-VFc), a high performanced bioanode was successfully developed. The GOx-based bioanode not only showed efficient electron transfer but also good catalytic activity toward glucose oxidation, whereas BOD assisted the reduction of O_2 at the poly(MMA-*co*-VFc)-coated cathode. Optimum conditions including polymer amount, temperature, and cell voltage were investigated to achieve the best performance. The resulting fuel cell produced a maximum power density of 323 $\mu W\ cm^{-2}$ with 10-mM glucose at 0.4 V in pH 7.4 phosphate buffer at room temperature. The design offers many advantages such as simplicity, low cost, the possibility of miniaturization, and long-term stability. In addition, the copolymer can be easily coated on a wide variety of surfaces, which are suitable for using in microelectronic devices.

ACKNOWLEDGEMENTS

This work was supported by the Scientific & Technological Research Council of Turkey (TUBITAK) under Grant 112Y100 and the Bulent Ecevit University Research Fund under Grant BEU-2013-77047330-01.

ORCID

Seyda Korkut https://orcid.org/0000-0003-2892-6182

REFERENCES

1. Yang X-Y, Tian G, Jiang N, Su B-L. Immobilization technology: a sustainable solution for biofuel cell design. *Energ Environ Sci*. 2012;5(2):5540-5563.
2. Chen J, Bamper D, Glatzhofer DT, Schmidtke DW. Development of fructose dehydrogenase-ferrocene redox polymer films for biofuel cell anodes. *J Electrochem Soc*. 2015;162:F258-F264.
3. Prasad KP, Chen Y, Chen P. Three-dimensional graphene-carbon nanotube hybrid for high-performance enzymatic biofuel cells. *ACS Appl Mater Interfaces*. 2014;6:3387-3393.
4. Milton RD, Hickey DP, Abdellaoui S, et al. Rational design of quinones for high power density biofuel cells. *Chem Sci*. 2015;6:4867-4875.
5. Fang L, Liu B, Liu L, Li Y, Huang K, Zhang Q. Direct electrochemistry of glucose oxidase immobilized on Au nanoparticles-functionalized 3D hierarchically ZnO nanostructures and its application to bioelectrochemical glucose sensor. *Sens Actuators B*. 2016;22:1096-1102.
6. Gutierrez-Sanchez C, Pita M, Vaz-Dominguez C, Shleev S, De Lacey AL. Gold nanoparticles as electronic bridges for laccase-based biocathodes. *J Am Chem Soc*. 2012;134:17212-17220.
7. Huang Y, Qin X, Li Z, et al. Fabrication of a chitosan/glucose oxidase-poly (anilineboronic acid)-Au (nano)/Au-plated Au electrode for biosensor and biofuel cell. *Biosens Bioelectron*. 2012;31:357-362.
8. Reuillard B, LeGoff A, Agnes C, et al. High power enzymatic biofuel cell based on naphthoquinone-mediated oxidation of glucose by glucose oxidase in a carbon nanotube 3D matrix. *Phys Chem Chem Phys*. 2013;15:4892-4896.
9. Scherbahn V, Putze MT, Dietzel B, Heinlein T, Schneider JJ, Lisdat F. Biofuel cells based on direct enzyme-electrode contacts using PQQ-dependent glucosedehydrogenase/bilirubin oxidase and modified carbon nanotube materials. *Biosens Bioelectron*. 2014;61:631-638.
10. O´Conghaile P, Pöller S, MacAodha D, Schuhmann W, Leech D. Coupling osmium complexes to epoxy-functionalised polymers to provide mediated enzyme electrodes for glucose oxidation. *Biosens Bioelectron*. 2013;43:30-37.

11. Yokoyama K, Lee SM, Tamiya E, et al. Mediated glucose sensor using a cylindrical microelectrode. *Anal Chim Acta*. 1992;263:101-110.
12. Merle G, Brunel L, Tingry S, et al. Electrode biomaterials based on immobilized laccase. Application for enzymatic reduction of dioxygen. *Mater Sci Eng C*. 2008;28:932-938.
13. Fabre B. Ferrocene-terminated monolayers covalently bound to hydrogen-terminated silicon surfaces. Toward the development of charge storage and communication devices. *Acc Chem Res*. 2010;43:1509-1518.
14. Morsbach J, Elbert J, Rüttiger C, Winzen S, Frey H, Gallei M. Polyvinylferrocene-based amphiphilic block copolymers featuring functional junction points for cross-linked micelles. *Macromolecules*. 2016;49:3406-3414.
15. Nunns A, Whittell GR, Winnik MA, Manners I. Crystallization-driven solution self-assembly of μ-ABC miktoarm star terpolymers with core-forming polyferrocenylsilane blocks. *Macromolecules*. 2014;47:8420-8428.
16. Tonhauser C, Mazurowski M, Rehahn M, Gallei M, Frey H. Water-soluble poly (vinylferrocene)-b-poly (ethylene oxide) diblock and miktoarm star polymers. *Macromolecules*. 2012;45:3409-3418.
17. Şen S, Uygun Gök A, Gülce H, Aldissi M. Synthesis and characterization of polyvinylferrocene/polypyrrole composites. *J Macromol Sci Part A: Pure Appl Chem*. 2008;45:485-494.
18. Saito T, Watanabe M. Characterization of poly (vinylferrocene-co-2-hydroxyethyl methacrylate) for use as electron mediator in enzymatic glucose sensor. *React Funct Polym*. 1998;37:263-269.
19. Şenel M, Abasıyanık MF. Construction of a novel glucose biosensor based on covalent immobilization of glucose oxidase on poly (glycidyl methacrylate-co-vinylferrocene). *Electroanalysis*. 2010;22:1765-1771.
20. Kuramoto N, Shishido Y, Nagai K. Preparation of thermally responsive and electroactive poly(N-acryloylpyrrolidine-co-vinylferrocene). *Macromol Rapid Commun*. 1994;15:441-444.
21. Koide S, Yokoyama K. Electrochemical characterization of an enzyme electrode based on a ferrocene-containing redox polymer. *J Electroanal Chem*. 1999;468:193-201.
22. Baldwin MG, Johnson KE. Free-radical polymerization of vinyl ferrocene. *J Polym Sci Part A-1:Polym Chem*. 1967;5:2091-2098.
23. Liu J, Zhang X, Pang H, Liu B, Zou Q, Chen J. High-performance bioanode based on the composite of CNTs-immobilized mediator and silk film-immobilized glucose oxidase for glucose/O_2 biofuel cells. *Biosens Bioelectron*. 2012;31:170-175.
24. Liu S, Sun Y. Co-immobilization of glucose oxidase and hexokinase on silicate hybrid sol–gel membrane for glucose and ATP detections. *Biosens Bioelectron*. 2007;22:905-911.
25. Maniruzzaman M, Jang SD, Kim J. Titanium dioxide-cellulose hybrid nanocomposite and its glucose biosensor application. *J Mater Sci Eng B*. 2012;177:844-848.
26. Dervisevic M, Custiuc E, Çevik E, Şenel M. Construction of novel xanthine biosensor by using polymeric mediator/MWCNT nanocomposite layer for fish freshness detection. *Food Chem*. 2015;181:277-283.
27. Zdarta J, Meyer AS, Jesionowski T, Pinelo M. A general overview of support materials for enzyme immobilization: characteristics, properties, practical utility. *Catalysts*. 2018;8:92-118.
28. Dwevedi A. *Enzyme Immobilization*. Switzerland: Springer International Publishing; 2016:132p.
29. Barton SC. 1D models for enzymatic biological fuel cells. *Electrochem Soc Interface Fall*. 2015;24:61-65.
30. Liang B, Guo X, Fang L, et al. Study of direct electron transfer and enzyme activity of glucose oxidase on graphene surface. *Electrochem Commun*. 2015;50:1-5.
31. Bard AJ, Faulkner LR. *Electrochemical Methods: Fundamentals and Applications*. New York: Wiley; 2001:864p.
32. Yu CM, Chen LC. Turning glucose and starch into electricity with an enzymatic fuel cell. *EAEF*. 2009;2:1-6.
33. Campbell AS, Murata H, Carmali S, Matyjaszewski K, Islam MF, Russell AJ. Polymer-based protein engineering grown ferrocene-containing redox polymers improve current generation in an enzymatic biofuel cell. *Biosens Bioelectron*. 2016;86:446-453.
34. Chen Y, Gai P, Zhang J, Zhu JJ. Design of an enzymatic biofuel cell with large power output. *J Mater Chem*. 2015; A3:11511-11516.
35. Pizzariello A, Stred'ansky M, Miertus S. A glucose/hydrogen peroxide biofuel cell that uses oxidase and peroxidase as catalysts by composite bulk-modified bioelectrodes based on a solid binding matrix. *Bioelectrochemistry*. 2002;56:99-105.
36. Liu Y, Dong S. A biofuel cell harvesting energy from glucose-air and fruit juice-air. *Biosens Bioelectron*. 2007;23:593-597.
37. Meredith MT, Kao D-Y, Hickey D, Schmidtke DW, Glatzhofer DT. High current density ferrocene-modified linear poly (ethylenimine) bioanodes and their use in biofuel cells. *J Electrochem Soc*. 2011;158:B166-B174.
38. Zhaoa HY, Zhoua HM, Zhanga JX, Zhenga W, Zheng YF. Carbon nanotube-hydroxyapatite nanocomposite: A novel platform for glucose/O2 biofuel cell. *Biosens Bioelectron*. 2009;25:463-468.
39. Haddad R, Mattei JG, Thery J, Auger A. Novel ferrocene-anchored ZnO nanoparticles/carbon nanotube assembly for glucose oxidase wiring: application to a glucose/air fuel cell. *Nanoscale*. 2015;7:10641-10647.
40. Valentine S, Mano N, Heller A. A four-electron O2-electroreduction biocatalyst superior to platinum and a biofuel cell operating at 0.88 V. *J Am Chem Soc*. 2004;126:8368-8369.
41. Güven G, Sahin S, Güven A, Yu EH. Power harvesting from human serum in buckypaper-based enzymatic biofuel cell. *Front Energy Res*. 2016;4. https://doi.org/10.3389/fenrg.2016.00004

SUPPORTING INFORMATION

Additional supporting information may be found online in the Supporting Information section at the end of the article.

How to cite this article: Korkut S, Kilic MS, Hazer B. Newly designed bioanode for glucose/O_2 biofuel cells to generate renewable energy. *Asia-Pac J Chem Eng*. 2019;e2374. https://doi.org/10.1002/apj.2374